JOURNAL OF VIROLOGY, Oct. 1995, p. 6367–6375 Vol. 69, No. 10
0022-538X/95/$04.00+0

Interaction of Polypyrimidine Tract-Binding Protein with the 5′ Noncoding Region of the Hepatitis C Virus RNA Genome and Its Functional Requirement in Internal Initiation of Translation

NAUSHAD ALI AND ALEEM SIDDIQUI*

Department of Microbiology and Program in Molecular Biology, University of Colorado Health Sciences Center, Denver, Colorado 80262

Received 9 May 1995/Accepted 12 July 1995

Initiation of translation of the human hepatitis C virus (HCV) RNA genome occurs by internal ribosome entry into the 5′ noncoding region (5′NCR) in a cap-independent manner. The internal ribosome entry site of the HCV 5′NCR has been previously defined to encompass almost the entire 5′NCR. Here we report the interaction of polypyrimidine tract-binding protein (PTB) at three distinct regions within the 5′NCR by UV cross-linking assays. All three regions contain a consensus polypyrimidine tract motif. The evidence for the interaction of recombinant PTB at multiple sites within the 5′NCR is based on the use of 5′NCR mutants as competitors and by direct UV cross-linking of the mutant RNAs. Furthermore, the PTB isomers from HeLa nuclear extracts interact with the HCV 5′NCR, as shown by immunoprecipitation of a UV cross-linked complex with anti-PTB serum. Immunodepletion of PTB from translation lysates suggested the functional requirement for PTB during translation initiation of the HCV RNA. Addition of purified PTB to immunodepleted lysates did not restore translation mediated by the HCV 5′NCR, indicating the requirement of PTB-associated factors that were removed during immunodepletion.

Human hepatitis C virus (HCV) is recognized as the principal causative agent of parenteral non-A, non-B hepatitis (for reviews, see references 20 and 37). HCV infection leads to chronic hepatitis in the majority of infected individuals (29). A strong link between HCV infection and development of hepatocellular carcinoma has been documented (43). On the basis of several criteria, including genome organization, molecular features, and biochemical properties, HCV has been classified as one of the genera of the *Flaviviridae* family (9, 23, 32, 41). The HCV genome is 9.4 kb long and has positive polarity, consisting of various lengths of 5′ noncoding region (5′NCR) (331 to 341 nucleotides [nt]), a long open reading frame encoding a polyprotein consisting of approximately 3,000 amino acids, and a short 3′NCR (20). The polyprotein is further processed into at least two structural and several nonstructural functionally active proteins (Fig. 1A).

While clinical isolates of the HCV genomes display considerable heterogeneity within the coding region, the 5′NCR is highly conserved (over 98% homology) (7, 17). A complex secondary structure has been proposed for the 5′NCR from phylogenetic comparative sequence analysis (6). There are multiple cryptic AUG codons within the 5′NCR. These features, coupled with experimental evidence derived from successful expression of the second cistron in the context of dicistronic expression vectors, strongly argue for the presence of an internal ribosome entry site (IRES) within the HCV 5′NCR (24, 42, 46). Kettinen et al. (24) further demonstrated a functional role of the coding region as a part of the IRES element located immediately 3′ distal to the initiator AUG. A detailed examination of the HCV IRES by extensive mutational analysis revealed the functional role of a helical structure associated with the pyrimidine tract II (previously defined as Py-I [47]) (Fig. 1B) and a probable pseudoknot structure located immediately upstream of the initiator AUG (45, 48). These secondary-tertiary interactions are essential *cis* elements of the HCV IRES (45, 48). Deletion and insertional mutagenesis studies suggest that almost the entire 5′NCR with the exception of 29 nt at the extreme 5′ end may constitute the HCV IRES element (48). Thus, the translational strategy used by HCV is similar to that employed by members of the family *Picornaviridae* (for reviews, see references 1, 31, and 38). On the basis of several features, the HCV IRES element appears to be similar to the type II IRES elements, in which IRES is located either immediately upstream of the initiator AUG or includes the AUG triplet (2, 21, 48). While the majority of the eukaryotic mRNAs are translated by a ribosome-scanning mechanism (25), IRES-mediated translation has been observed for a few cellular mRNAs (27, 31). These observations further suggest that eukaryotic translation machinery can support cap-independent translation.

Among the various cellular *trans*-acting factors, the polypyrimidine tract-binding protein (PTB), also known as heterogeneous nuclear ribonucleoprotein I or p57 (13, 14, 22), principally involved in splicesome assembly (5, 15, 33), has been shown to be functionally required for internal initiation of translation by picornaviruses (12, 22, 26, 36). PTB binds to picornavirus IRES elements at one or more sites (18, 26, 49), and its removal from cellular extracts abrogates translation initiation of picornavirus RNA but not β-globin mRNA (3, 19, 34).

In this study, we investigated the possibility of PTB binding within the HCV 5′NCR. UV cross-linking assays carried out with recombinant PTB clearly demonstrated the interaction of PTB with 5′NCR at at least three distinct sites. Our studies performed with PTB derived from HeLa nuclear lysates also

* Corresponding author. Mailing address: Department of Microbiology, B172, University of Colorado Health Sciences Center, 4200 E. 9th Ave., Denver, CO 80262. Phone: (303) 270-7016. Fax: (303) 270-8330.

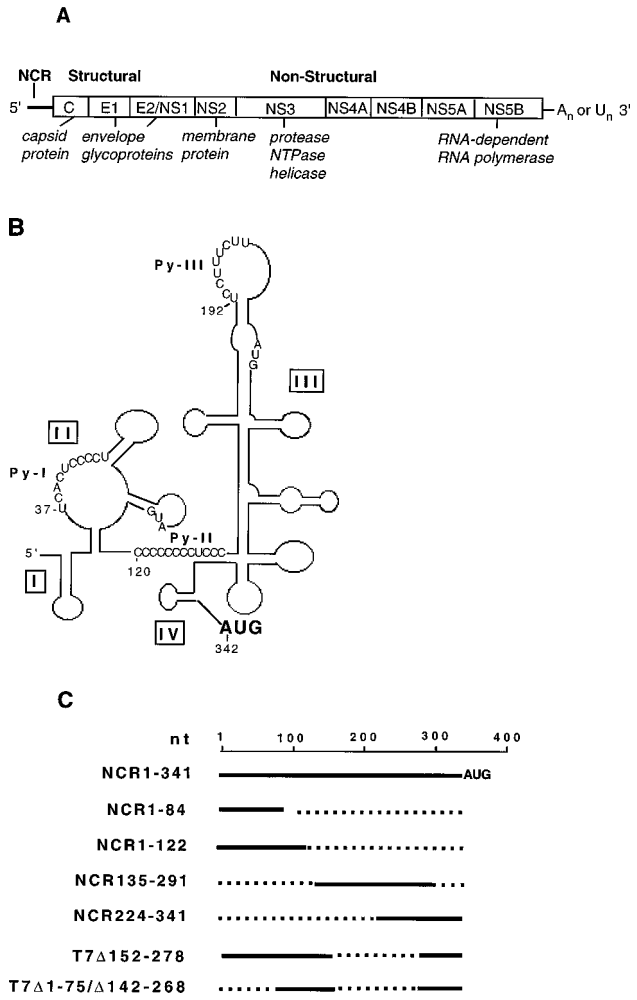

FIG. 1. (A) Genomic organization of the HCV RNA and polyprotein processing scheme. (B) Schematic representation of computer-generated RNA secondary structure of the 5′NCR (adapted from Brown et al. [6]). The locations of the pyrimidine tracts (Py-I, Py-II, and Py-III) and the four structural domains within the open box are shown. (C) Maps of HCV 5′NCR deletion mutants. Dotted lines represent the extent of deletion. The nucleotide position (nt) indicates the first nucleotide of the mutants.

show PTB's interaction with the HCV 5′NCR, as evidenced by immunoprecipitation with a monoclonal antiserum directed against PTB. Furthermore, the immunodepletion of PTB from translation lysates completely inhibited the translational capacity of 5′NCR. These studies suggest that PTB plays a functional role in the internal initiation of the HCV RNA genome.

MATERIALS AND METHODS

Construction of recombinant plasmids. The construction of plasmid pGEM5′NC, which contains the full-length 5′NCR of HCV-I, has been described previously (46). NCR135-291, which represents domain III of the 5′NCR, was PCR amplified from pGEM5′NC with sense (5′CGGGAATTCAGAGC CATAGTG3′) and antisense (NC/AS [5′AGGCGGATCCAGTACCACAAG G3′]) primers. The amplified product was cloned at *Eco*RI-*Bam*HI sites in pGEM-3. Nucleotides 224 to 341 of 5′NCR were amplified from plasmid pGEM5′NC with sense (5′TGGAAGCTTAGATTTGGGCGTG3′) and antisense (NC/AS) primers and cloned at *Hin*dIII-*Sac*I sites in pGEM-4 to construct NCR224-341. Plasmid T7C75-332 represents the 5′NCR of HCV-II, in which the upstream 75 nt have been deleted (46). The *Age*I-*Stu*I fragment was deleted from this plasmid to construct the mutant T7CΔ1–75/Δ142–268 plasmid. All of the plasmids generated for this study are listed in Fig. 1C. Construction of the plasmids pHC5NC/126, pHC5NC/121/126/319, and T7CΔ152–278 has been described previously (47).

In vitro transcription. Plasmid DNAs were purified by the CsCl density gradient centrifugation method. pGEM5′NC was linearized with *Eco*RI and transcribed in vitro with T7 RNA polymerase to produce full-length HCV 5′NCR RNA (NCR1-341). NCR1-84 and NCR1-122 RNAs were prepared similarly by digestion of pGEM5′NC with *Nco*I and *Sma*I, respectively. Plasmids pHC5NC/126 and pHC5NC/121/126/319 were linearized with *Xba*I, and RNA was synthesized with SP6 RNA polymerase. T7CΔ152–278 and T7CΔ1–75/Δ142–268 were digested with *Xba*I to linearize them before transcription with T7 RNA polymerase. Plasmids NCR135-291 and NCR224-341 were linearized with *Bam*HI and *Nco*I, respectively, and transcribed with T7 RNA polymerase. Plasmid pT7-GEM-Polio(N) containing the full-length poliovirus (Mahony) cDNA was digested with *Msc* 1, which cleaves the DNA at nt 627, for use in UV cross-linking studies (see Fig. 5A). The same plasmid was also digested with *Bam*HI (nt 220) to generate poliovirus NCR1-220 RNA for the competition studies described in the legend to Fig. 2C. The poliovirus RNAs were synthesized by T7 RNA polymerase. Plasmid T7C1-341 was linearized with *Hpa*I and transcribed with T7 RNA polymerase. All of the DNA templates, after digestion with the appropriate restriction enzyme, were purified by elution of the desired fragment from the agarose gels before transcription. The radioactive RNA probes were synthesized under similar reaction conditions with 4-thio-UTP and [^{32}P]CTP.

Expression of recombinant PTB. The plasmid GST-2TK/PTB, which encodes the glutathione *S*-transferase (GST)–PTB fusion protein, was a generous gift of M. A. Garcia-Blanco. The expression of GST-PTB was induced with 1 mM IPTG (isopropyl-β-D-thiogalactopyranoside) in *Escherichia coli* (JM101) cells and affinity purified on glutathione-Sepharose beads (Pharmacia). The final preparation was dialyzed against 5 mM HEPES (*N*-2-hydroxyethylpiperazine-*N*′-2-ethanesulfonic acid [pH 7.6])–1 mM EDTA–1 mM dithiothreitol–0.2 mM–phenylmethylsulfonyl fluoride–10% (vol/vol) glycerol. GST was also purified by a similar procedure and used as a control.

UV cross-linking of RNA with proteins. 4-Thio-UDP (Sigma) was phosphorylated with nucleoside 5′-diphosphate kinase to prepare 4-thio-UTP according to the method of Stade et al. (39). The 4-thio-UTP and [^{32}P]CTP were included in an in vitro transcription reaction mixture to produce thio-U-containing ^{32}P-labeled RNA. Protein samples were incubated with RNA probe for 30 min at 30°C in an RNA binding buffer (5 mM HEPES [pH 7.6], 25 mM KCl, 2 mM $MgCl_2$, 0.1 mM EDTA, 10 mM dithiothreitol, 15% [wt/vol] glycerol). Yeast tRNA (10 μg) and 40 U of RNasin (Promega) were also included in each reaction mixture (15 to 20 μl). Samples were irradiated with UV light (312 nm) for 30 min with a UV Stratalinker model 1800 (Stratagene) at 4°C. Unbound RNA was digested with 10 U of RNase A (U.S. Biochemical Corp.) for 15 min. Samples were analyzed by sodium dodecyl sulfate-polyacrylamide gel electrophoresis (SDS-PAGE) [10% polyacrylamide]) followed by autoradiography. In all of the competition assays, appropriate competitor RNAs were added along with other components of the reaction mixture prior to UV cross-linking.

Purification of PTB from HeLa nuclear extracts. Nuclear extracts from cultured cells were prepared essentially as described by Dignam (11). The final preparation was dialyzed against buffer D (20 mM HEPES-NaOH [pH 7.9], 20% [vol/vol] glycerol, 100 mM KCl, 0.2 mM EDTA, 0.5 mM dithiothreitol, 0.5 mM phenylmethylsulfonyl fluoride). Purification of p57/PTB was carried out according to the modified method of Gil et al. (15). One milliliter of slurried poly(U)-Sepharose 4B (Pharmacia), preequilibrated with buffer E (buffer D plus 0.05% Nonidet P-40 and 2.0 mM $MgCl_2$) was mixed with 1.5 mg of nuclear extracts and incubated at 4°C on a rotary shaker for 1 h. The mixture was loaded on a minicolumn, and the unbound materials were washed with buffer E containing 0.5 M KCl after the slurry had completely settled. The bound proteins were eluted with 0.8 M KCl added to the same buffer. Fractions were collected, and the protein concentration was determined. Fractions were dialyzed against buffer D, and PTB binding activity was determined by a UV cross-linking method.

Immunoprecipitation of the PTB-HCV 5′NCR complex. The ribonucleoprotein complexes formed between HCV 5′NCR RNA and partially purified HeLa PTB were prepared as described above. After UV cross-linking and RNase treatment, samples were diluted to 500 μl in buffer containing 50 mM Tris-HCl (pH 7.4), 5 mM EDTA, 1 mM dithiothreitol, 100 mM NaCl, 0.05% Nonidet P-40). Monoclonal anti-PTB antibody 7G12 (a generous gift of Gideon Dreyfuss) was added, and the mixture was incubated for 1 h at 4°C. Ten micrograms of anti-mouse immunoglobulin G (IgG) antibody (Sigma) was added, and immunocomplexes were immobilized on protein A-Sepharose beads (Pharmacia) and washed four times with the same buffer. The bound proteins were analyzed by SDS-PAGE followed by autoradiography.

Immunodepletion of PTB from cell lysates. For immunodepletion of PTB from the cell-free translation system, 8 μl of 7G12 antibody was added to 50 μl of rabbit reticulocyte lysate (RRL [Promega]) or HeLa S10 extract and incubated for 1 h at 4°C. Protein G-Sepharose (Pharmacia) was added, and the mixture was incubated further for an additional hour at 4°C on a rotary shaker. The mixture was centrifuged, and the supernatant was used for translation.

In vitro translation. The translation reactions were performed with RRLs. Proteins were radiolabeled with Trans-^{35}S label (ICN Biomedicals) and analyzed by SDS-PAGE. Luciferase activity in the RRLs was measured according to the method of de Wet et al. (10). Immunodepleted RRL and HeLa S10 fractions

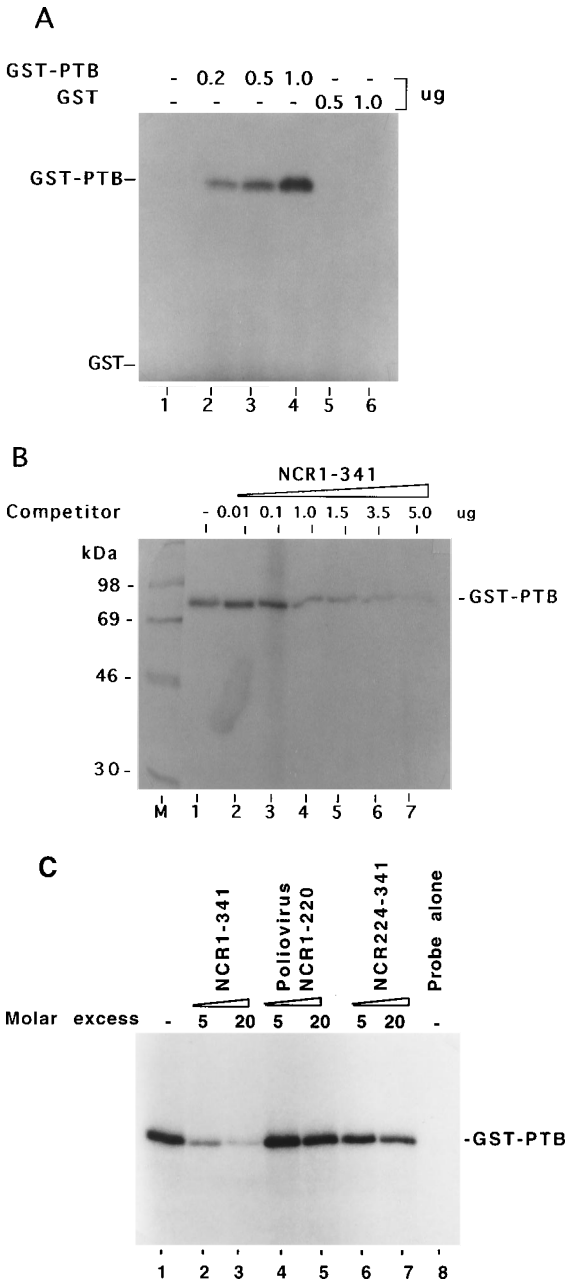

FIG. 2. UV cross-linking of the GST-PTB fusion protein with 5′NCR of HCV RNA (NCR1-341) followed by SDS-PAGE (10% polyacrylamide). (A) Interaction of GST-PTB with the full-length wild-type HCV 5′NCR RNA probe. Lanes: 1, probe alone; 2 to 4, increasing amounts of GST-PTB; 5 and 6, UV cross-linking of GST with the probe. (B) Interaction of PTB with HCV 5′NCR with increasing amounts of unlabeled homologous RNA used as competitor (lanes 2 to 7). GST-PTB (0.5 μg) was UV cross-linked to ~10^5 cpm of the NCR1-341 RNA probe. The 5′NCR RNA probe was synthesized in vitro with 4-thio-UTP and [^{32}P]CTP under standard conditions. Lane 1 contained no competitor. (C) Effects of competitors on PTB binding to the HCV 5′NCR RNA in UV cross-linking reactions. Lanes: M, molecular mass markers; 1, without competitor; 2 and 3, NCR1-341; 4 and 5, poliovirus 5′NCR representing nt 1 to 220; 6 and 7 NCR224-341; 8, probe alone. UV cross-linking of wild-type HCV 5′NCR thio-U-containing ^{32}P-labeled RNA probe with GST-PTB (80 ng) was carried out as described above. RNA competitors in 5 and 20 molar excess of the probe concentration were included in the reaction mixtures in the competition assay.

were supplemented with various amounts of recombinant PTB. The reconstituted lysates were also used for translation of T7C1-341 RNA.

RESULTS

Binding of PTB to the HCV 5′NCR. There are at least three potential pyrimidine-rich tract motifs located within the HCV 5′NCR. They are located at nt 37 to 46 (Py-I), 120 to 131 (Py-II), and 192 to 199 (Py-III) as shown in Fig. 1B. Py-I and Py-III sequences are part of single-stranded regions, but Py-II sequences are partially base paired with nt 319 to 324 (Fig. 1B) (6). The putative Py sequences of the HCV 5′NCR may serve as potential binding sites for PTB. We investigated the interaction of recombinant PTB with the HCV 5′NCR by UV cross-linking assays. The RNA probe was enzymatically synthesized in the presence of [^{32}P]CTP and 4-thio-UTP. The radiolabeled thio-U-containing 5′NCR probe was incubated with purified GST-PTB or GST at various protein concentrations. The reaction mixtures were subsequently UV irradiated and digested with RNase A prior to fractionation by SDS-PAGE. Appearance of a radioactive protein band in this analysis is due to the covalent interaction between ^{32}P-labeled probe and PTB. A radiolabeled PTB-RNA complex was formed between GST-PTB and the HCV 5′NCR, and the intensity of this complex increased as a function of protein concentration (Fig. 2A, lanes 2 to 4). However, under similar binding conditions, GST alone was not cross-linked to the probe (lanes 5 and 6). These results show interaction of 5′NCR with the PTB moiety in the GST-PTB fusion protein. The binding specificity of PTB to 5′NCR was confirmed by a competition assay (Fig. 2B). Various concentrations of unlabeled homologous RNA (NCR1-341) were added to the reaction mixture before UV cross-linking. The binding of PTB to the probe was considerably inhibited in the presence of unlabeled 5′NCR RNA (lanes 4 to 7). These results indicate the specificity of PTB's interaction with HCV 5′NCR. The interaction of the wild-type HCV 5′NCR with PTB was then compared with that of a heterologous RNA derived from nt 1 to 220 of poliovirus 5′NCR and a homologous RNA representing nt 224 to 341 (NCR224-341) of HCV 5′NCR in a competition assay. The results of this experiment are presented in Fig. 2C. With similar molar excess of the competitors, while unlabeled NCR1-341 RNA completely inhibited the PTB interactions with the RNA probe (lanes 2 and 3), poliovirus-derived RNA (lanes 4 and 5) failed to compete. Similarly, the HCV mutant RNA (NCR224-341), devoid of all of the Py motifs (Py-I, -II, -III), was unable to inhibit PTB interaction with the full-length HCV 5′NCR RNA (lanes 6 and 7). These observations confirm the specificity of PTB binding with HCV 5′NCR.

Mapping of PTB binding sites in HCV 5′NCR. Our mapping strategy involved the use of several mutant 5′NCR RNAs both in direct binding to PTB and as unlabeled competitors in the UV cross-linking of the wild-type 5′NCR. In the first analysis, the T7CΔ152–278 thio-U-containing deletion mutant RNA was used as a probe. This deletion essentially eliminates the upper portion of domain III, including the apical loop containing the Py-III motif. The enhancement of the probe transfer signal as a result of PTB binding to the labeled RNA was evident with increasing concentrations of the protein (Fig. 3A, lanes 2 to 4). Notably, the intensity of the binding signal was reduced considerably when unlabeled homologous competitor RNA was added to the reaction mixture (lanes 5 and 6). The binding specificity of PTB was further confirmed in a competition assay in which wild-type NCR1-341 RNA probe was used for UV cross-linking with PTB in the presence of unlabeled T7CΔ152–278 RNA (Fig. 3B). The competitor RNA drasti-

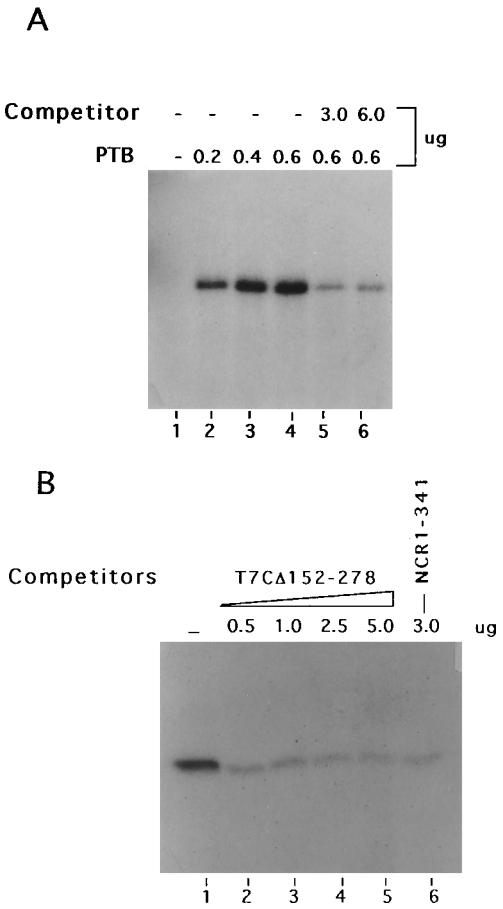

FIG. 3. Binding of GST-PTB with HCV 5′NCR RNA probe lacking domain III sequences. (A) UV cross-linking of T7CΔ152–278 RNA probe with increasing amounts of PTB (lanes 2 to 4). Lane 1 contained probe alone, and lanes 5 and 6 show specific inhibition of PTB binding with the probe by unlabeled homologous RNA. The UV cross-linked fractions were subjected to SDS-PAGE (10% polyacrylamide). (B) Inhibitory effect of heterologous competitor T7CΔ152–278 on the interaction of GST-PTB with the NCR1-341 RNA probe. The reaction mixtures were fractionated by SDS-PAGE. Lanes: 1, no competitor; 2 to 5, increasing amounts of competitor RNA; 6, homologous competitor.

cally inhibited the interaction between PTB and wild-type 5′NCR1-341 (lanes 2 to 5). The unlabeled competitor wild-type 5′NCR RNA is included as a positive control, which as expected abolished the PTB-RNA complex (lane 6). These results together suggest that both Py-I and Py-II motifs along with other structural elements may be potential sites of PTB interaction. The mutant T7CΔ152–278 HCV 5′NCR is devoid of the Py-III motif but retains both Py-I and Py-II, including the helical element (Fig. 1B).

To further identify these regions as PTB binding sites, we used two candidate RNA probes along with the wild-type 5′NCR. First, a truncated RNA representing nt 1 to 122 from the extreme 5′ end, which includes a pyrimidine-rich tract (Py-I; nt 37 to 46) was used. PTB binding to this sequence is efficient (Fig. 4A, lanes 4 and 5) and is comparable to that of the wild-type 5′NCR (lane 1). Next, we selected a mutant pHC5NC/126 RNA in which four pyrimidines of the Py-II tract (nt 126 to 129) were altered to purines (47). These nucleotide changes essentially disrupt the helical interaction between nt 126 to 134 and nt 315 to 323. Although this mutation dramatically affects translation initiation (47), it has no effect on PTB binding (Fig. 4A, lanes 2 and 3). The specific binding of PTB to the nt 1 to 122 sequence of 5′NCR was further substantiated by the use of several unlabeled RNAs encompassing that sequence. These include homologous NCR1-122, NCR1-84, and the wild-type 5′NCR RNAs. In all cases, the level of interaction between PTB and the NCR1-122 probe was reduced (Fig. 4B). Binding of these RNAs to PTB unambiguously defines the presence of a PTB binding site within nt 1 to 84, which is designated as PTB site I.

NCR135-291 RNA, which represents the largest stem-loop structure of domain III, was used as a competitor in UV cross-linking of PTB with the full-length wild-type 5′NCR. The results of competitive inhibition are shown in Fig. 4C (lanes 2 to 4). Effective competition by the unlabeled NCR135-291 RNA was obtained at all concentrations, suggesting the presence of a PTB binding site within that sequence. Located within this sequence at nt 192 to 200 is a characteristic pyrimidine-rich sequence followed by a noninitiator AUG, designated here as PTB site II.

A double-deletion mutant RNA, NCRΔ1–75/Δ142–268, was constructed in which the pyrimidine-rich motif (Py-II; nt 120 to 131) was linked to the primary sequences required to form the helical structural elements at the 3′ border of wild-type 5′NCR. This RNA was found to compete with wild-type 5′NCR for PTB binding (Fig. 4C, lanes 5 to 7). The competitive binding achieved by this mutant further established that PTB site III was within the HCV 5′NCR located in the 3′ border region of the IRES. We cannot rule out the possibility that this mutant may not have formed the native helical structure because of a large deletion. It is evident that a larger amount of competitor was needed to achieve the diminution of PTB binding (compare lanes 2 and 3 with lanes 5 and 6 in Fig. 4C).

In another approach, a double compensatory mutant RNA, pHC5NC/121/126/319 (47), was used as a probe. This mutant is similar to pHC5NC/126, except that the helical structural region at the Py-II tract was restored by the introduction of mutations in the complementary sequences and two more pyrimidine residues at nt 122 and 123 were mutated to purines. With these rearrangements of nucleotide sequences, the mutant contains the same structure as the wild type, but 60% of the pyrimidine residues in Py-II are altered to purines (47). This mutant translates efficiently both in vitro and in vivo. In this analysis, a constant amount of GST-PTB was used while increasing amounts of the 4-thio-U-containing ^{32}P-labeled mutant probe were added. The intensity of the radiolabeled PTB signal correlates with the amount of probe added to the reaction mixture (Fig. 4D). Thus, a functionally active mutant HCV 5′NCR retains its capacity to bind PTB despite the fact that only 40% of the pyrimidine residues were present in the Py-II motif.

In summary, the results of this detailed analysis identify three noncontiguous binding regions of PTB within the HCV 5′NCR, designated as sites I, II, and III. Interestingly, all of these regions contain characteristic stretches of pyrimidine-rich tracts (Fig. 1B).

Interaction of cellular PTB with the HCV 5′NCR. The PTB binding studies described above were carried out with a bacterially expressed GST fusion protein. To demonstrate the interaction of PTB from cell lysates with the HCV 5′NCR, partially purified HeLa nuclear proteins were used. The purified protein fraction was subjected to a UV cross-linking assay with the RNA probes transcribed from wild-type HCV 5′NCR. The poliovirus 5′NCR RNA probe, known to efficiently bind HeLa PTB (19, 34), was included as a positive control. Two closely migrating ribonucleoprotein complexes with an average molecular mass of 57 kDa (p57) were resolved as major bands

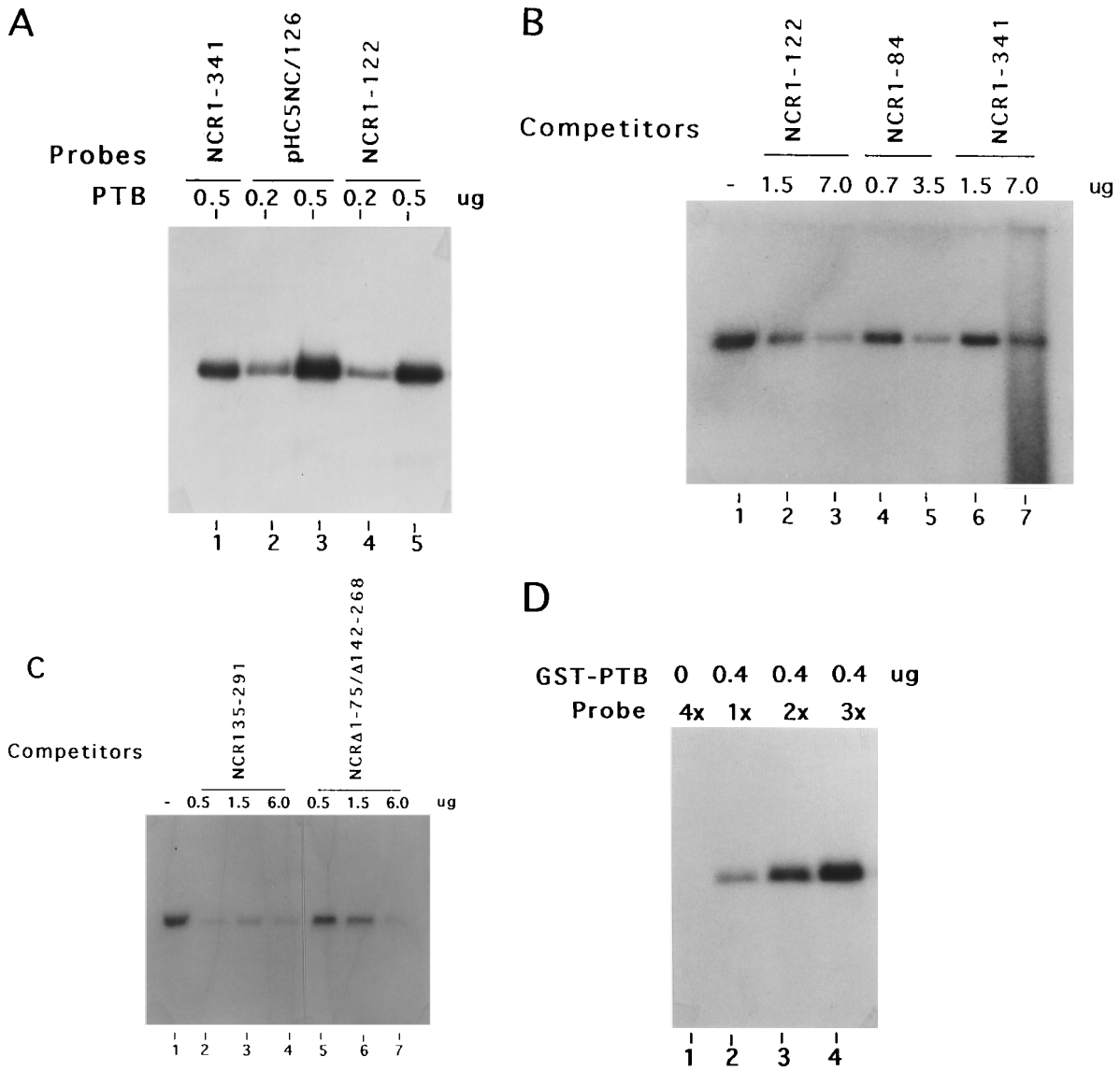

FIG. 4. Mapping of PTB binding sites in the HCV 5′NCR. All of the NCR RNA probes contained 4-thio-U and were ^{32}P labeled. The UV cross-linked RNA-protein complexes were subjected to SDS-PAGE (10% polyacrylamide). (A) Direct binding of HCV 5′NCR mutant RNA probes. UV cross-linking was carried out with the labeled probes at the indicated amounts of GST-PTB. Lanes: 1, NCR1-341 RNA; 2 and 3, pHC5NC/126 RNA probe. In this mutant (pHC5NC/126), Py-II sequences are mutated to purines, leading to disruption of the helical structure (47). Lanes 4 and 5 contained the NCR1-122 RNA probe, which contains the putative Py-I motif and represents the 5′ end sequences of the NCR. (B) Binding of PTB with the NCR1-122 RNA probe in the presence of unlabeled competitor NCR mutants. Lanes: 1, no competitor; 2 and 3, NCR1-122 RNA; 4 and 5, NCR1-84 RNA; 6 and 7, NCR1-341 RNA. (C) Competitive inhibition of PTB binding to the wild-type NCR1-341 RNA probe by deletion mutant 5′NCR RNAs. Lanes: 1, no competitor; 2 to 4, increasing amounts of NCR135-291 (contains domain III of the HCV 5′NCR); 5 to 7, increasing amounts of NCRΔ1–75/Δ142–268 (contains Py-II and downstream sequences involved in a probable pseudoknot structure) (45). (D) Direct binding of a double compensatory mutant, pHC5NC/121/126/319, RNA probe to PTB. Increasing amounts of probe ($1\times = 1.6 \times 10^4$ cpm) were used for the UV cross-linking, while the amount of GST-PTB was kept constant.

(Fig. 5A, lane 1). These complexes also correspond to the cross-linked products of the poliovirus RNA probe (lane 3). The cross-linking specificity of the p57 complex was confirmed by addition of unlabeled homologous competitor RNA under the same reaction conditions. The interaction of p57 doublets with HCV probe was considerably abolished by the unlabeled homologous competitor (lane 2), clearly indicating the specific interaction of these proteins with the HCV 5′NCR. In this analysis, two additional protein bands, 72 and 110 kDa, also show a relatively weaker but specific interaction with the RNA probes. A few low-molecular-mass species were cross-linked with the poliovirus 5′NCR but not with the HCV 5′NCR. This is consistent with previous observations in which smaller polypeptides selectively interact with the 5′NCRs of picornaviruses (8, 12). With a similar approach, the purified p57 proteins were UV cross-linked with the HCV 5′NCR and subsequently immunoprecipitated with a monoclonal anti-PTB antibody (7G12). The results of this analysis, shown in Fig. 5B, lane 2, identify the p57 doublet UV cross-linked with HCV 5′NCR as PTB. In contrast, immunoprecipitation was not observed with unrelated serum (lane 1). These observations unambiguously demonstrate that the cellular p57 complex of PTB proteins interacts directly with the HCV 5′NCR. This complex of protein bands ranging from 57 to 62 kDa in size represents isomers

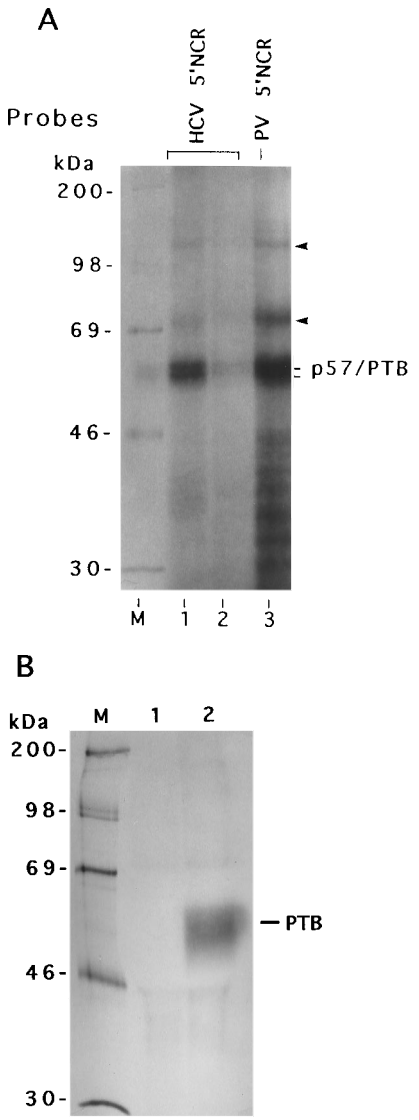

FIG. 5. Interaction of cellular PTB with the 5′NCR of HCV. (A) A 0.5-μg aliquot of protein fraction purified with poly(U)-Sepharose 4B matrix from HeLa nuclear extracts was UV cross-linked with the HCV 5′NCR (NCR1-341) ^{32}P-labeled RNA probe (lane 1). Unlabeled homologous RNA (5.0 μg) was included as a competitor (lane 2) in the reaction mixture during UV cross-linking. Poliovirus (PV) 5′NCR RNA (lane 3) was used as an RNA probe to UV cross-link similar protein fractions. M, molecular mass standard. Two RNA-protein bands located at 72 and 110 kDa are indicated by arrowheads. (B) Immunoprecipitation of HeLa PTB UV cross-linked to the wild-type 5′NCR. An affinity-purified fraction was used in UV cross-linking as described above. A monoclonal anti-PTB antibody, 7G12 (lane 2), was used to immunoprecipitate the UV cross-linked fractions (normal serum [lane 1]).

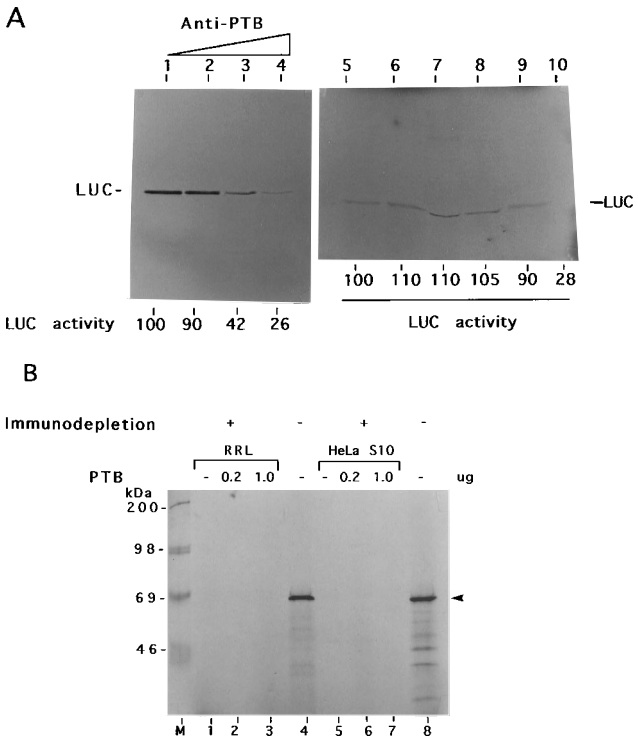

FIG. 6. (A) Inhibition of HCV IRES-mediated translation of the luciferase gene (LUC) by monoclonal anti-PTB serum. Increasing amounts of anti-PTB serum (lanes 2 to 4, 0.1, 1.0, and 2.0 μl, respectively) were added to the translation mixture. Lane 1 contained no anti-PTB serum. In another set of experiments, 1 and 2 μl of normal rabbit serum (lanes 6 and 7, respectively) or 2 and 4 μg of anti-mouse IgG (lanes 8 and 9, respectively) were added to the translation mixture. Lane 5 contained no serum, and in lane 10, 2 μl of anti-PTB serum served as a control. The in vitro-transcribed T7C1-341 RNA was translated in RRLs in the presence of Trans-^{35}S label and analyzed by SDS-PAGE (10% polyacrylamide) followed by autoradiography. The percentage of luciferase activity in the antibody-containing samples was normalized against that of the control without antibody (lane 1). (B) Translation of HCV IRES-mediated luciferase in the PTB-immunodepleted RRL and HeLa lysates. The indicated amounts of GST-PTB were added to the lysates. Translation of T7C1-341 RNA in immunodepleted RRLs and HeLa S10 cell fractions is shown in lanes 1 to 3 and 5 to 7, respectively. The immunodepleted lysates were supplemented with recombinant PTB (lanes 2, 3, 6, and 7). Lanes 1 and 5 were without exogenous PTB. Lanes 4 and 8 show translation in native (not antibody treated) RRLs and HeLa S10 cell fractions, respectively, under similar assay conditions. Luciferase is indicated by an arrowhead.

of PTB (5, 13, 33). These results are consistent with those from experiments conducted with picornavirus 5′NCRs (18, 49).

Effect of PTB on HCV IRES-mediated translation initiation. In this study, the functional role of PTB interaction with the HCV 5′NCR was examined. The plasmid T7C1-341, in which a full-length HCV 5′NCR was cloned in front of the luciferase gene such that the translation of the reporter gene is dictated by the HCV IRES, was used (46). The transcripts were translated in RRLs in the presence of various amounts of a monoclonal anti-PTB antibody, 7G12. The translational efficiency of the luciferase was progressively inhibited by the addition of increasing amounts of antibody (Fig. 6A, lanes 2 to 4). In contrast, addition of unrelated antibodies such as anti-mouse IgG (lanes 8 and 9) or a normal rabbit serum (lanes 6 and 7) did not show any inhibitory effect on the cap-independent translation. These results provide evidence that the role of PTB is functionally indispensable in the HCV IRES-mediated translation. The role of PTB in the HCV IRES-mediated translation was further determined by PTB immunodepletion-reconstitution experiments. HeLa S10 fraction and RRLs capable of efficient translation of T7C1-341 RNA were immunodepleted with anti-PTB serum. These lysates were then used for translation of T7C1-341 LUC transcripts. The results show that PTB-depleted lysates were incapable of translating luciferase RNA (Fig. 6B, lanes 1 and 5). The IRES-mediated translation could not be restored after addition of exogenous PTB to the immunodepleted lysates (lanes 2, 3, 6, and 7), suggesting the requirement of cellular factors associated with PTB.

DISCUSSION

PTB has been shown to play an important role in spliceosome assembly of the eukaryotic pre-mRNAs and in cap-inde-

pendent translation initiation of picornaviruses (3, 13–15, 18, 19, 26). Translation of HCV RNA is also initiated by cap-independent internal ribosome binding to the 5′NCR. Important features of the HCV 5′NCR include a complex secondary structure (6) containing potential pyrimidine-rich tracts at more than one location, the presence of multiple noninitiator AUG triplets, a probable pseudoknot structure at the 3′ border of the IRES element, and the requirement of nearly the entire 5′NCR for IRES function. Experimental results accumulated in several laboratories which identified these structural features provide conclusive evidence for the IRES-mediated translation of the HCV RNA genome (24, 42, 45–48).

Among picornaviruses, there is ample evidence that internal initiation of translation is facilitated by interactions of cellular and or viral proteins (3, 16, 22, 28). However, one of the unsolved questions is whether IRES function requires factors other than those involved in translation initiation of eukaryotic mRNAs. Identification of additional factors required for internal initiation of translation has been the topic of intense investigation. Of the several *trans*-acting cellular factors, two factors, p57/PTB and La autoantigen (40), have gained prominence in the recent past. In this study, we have investigated the binding of PTB to the 5′NCR of the HCV. The evidence presented here shows that PTB, which binds picornavirus 5′NCRs at multiple sites (18), also binds the HCV 5′NCR and is functionally required for internal initiation of translation. Although PTB interacts with three noncontiguous regions of the HCV 5′NCR, exact sequences including the Py motif or the structural elements with which PTB makes contact could not be determined. Of interest in this respect, is a double compensatory mutant, pHC5NC/121/126/319, in which about 60% of the pyrimidines (Py-II) were altered to purines, which maintained the PTB interaction, suggesting that PTB binding may be focused more on structural motifs than on the pyrimidine-rich sequence per se. This is not without precedent, because PTB binding has been shown to occur in a pre-mRNA element that does not contain a pyrimidine tract (30). Furthermore, in another study, a pyrimidine homopolymer was unable to displace PTB binding (19). On the basis of their detailed examination of the sites of PTB binding in picornavirus 5′NCRs, Witherall et al. (49) suggested that common features of PTB binding include such structural features as helix–single-stranded RNA–helix. Further studies will be needed to define the exact sites and the primary and structural components of PTB binding sites in the HCV 5′NCR.

The HCV 5′NCR contains three independent binding sites for PTB comprising all or part of nt 1 to 84 (site I), nt 135 to 291 (site II), and site III, which includes a helical structure encompassing nt 126 to 134 (base paired with nt 315 and 323) located in the vicinity of initiator AUG. Among the three PTB binding sites in the poliovirus 5′NCR, one is located within the pyrimidine tract while the others are identified as non-pyrimidine stem-loop or helical structures (18). In the UV cross-linking and competition assay, PTB binding site I (1 to 75 nt) in the HCV 5′NCR appears to interact with a relatively higher affinity (Fig. 4B). These sequences contain a putative pyrimidine-rich motif (Py-I, beginning at nt 37 to 46) with a noninitiator AUG located at nt 85 farther downstream, but a long stem may bring the triplet in close structural proximity to the Py sequences and thus may constitute a characteristic Yn-Xm-AUG motif. Additional features of site I include a stem and single-stranded region followed by a second stem. Such structural features have been previously defined for picornavirus encephalomyocarditis virus 5′NCR (49, 50) (Fig. 1B). Earlier studies from this laboratory showed that deletion of this region markedly reduced the translational efficiency of the HCV IRES (46). Interestingly, an antisense oligonucleotide directed against sequences between nt 38 and 65, which overlaps the putative Py-I sequence, blocked HCV RNA translation (44). These observations support the functional importance of this 5′ upstream region.

The region in which PTB binding site II is located contains the largest stem-loop structure, or domain III as defined by Brown et al. (6). A characteristic pyrimidine-rich sequence motif, Yn-Xm-AUG, is located in the apical loop of the domain, followed by a noninitiator AUG triplet 17 nt downstream. Previous studies from this laboratory in which pyrimidine residues and the AUG codon were mutated did not lead to any appreciable decrease in the translational efficiency of the 5′NCR (47). However, a major deletion of 127 nt, which essentially eliminates the upper portion of this domain including the Py-III tract, had detrimental effects on IRES-mediated translation initiation (47). In the present analysis, PTB binding to an RNA derived from this region (NCR135-291) was maintained.

The third *cis* element (site III) that is identified as a PTB binding site represents a higher-order structure consisting of secondary and tertiary interactions. First, a highly conserved sequence maintains a helical structure in which nt 126 to 131 are base paired with nt 311 to 319. Disruption of this helical interaction resulted in a dramatic reduction in translation initiation (47). This mutant RNA did compete for PTB binding to the wild-type 5′NCR (data not shown). A compensatory mutation in which pyrimidine residues in nt 121 to 131 were altered to purines (about 60%), but with a complementary strand which contained a mutation restoring base pairing in these sequences, recovered translational efficiency of the 5′NCR. UV cross-linking of this RNA molecule with PTB was also observed in the present analysis (Fig. 4D). Further biochemical and genetic analysis of this region supports the existence of a pseudoknot structure in this region (45). These structural elements may serve as recognition sites for RNA-protein interactions including PTB. Thus, the HCV IRES resembles the IRES elements of picornaviruses in terms of the presence of the multiple *cis* elements involved in PTB interaction (4, 18, 26, 34).

UV cross-linking of the HCV 5′NCR with the PTB partially purified from HeLa cellular lysates revealed two closely migrating species with molecular masses ranging from 57 to 62 kDa. These isomers of PTB cross-linked to 5′NCR, were confirmed by the use of monoclonal anti-PTB serum (Fig. 5B). This pattern is consistent with previous studies of PTB complex interactions with cellular pre-mRNA and picornavirus 5′NCR (3, 14, 30).

Indirect evidence suggests that p57/PTB is an essential factor in translation of picornavirus mRNA (19, 22, 34). This conclusion is based on observations that specific anti-PTB serum inhibited cap-independent translation but not cap-dependent translation (19). Using a similar approach, we investigated the functional role of PTB in HCV IRES-dependent translation. Addition of monoclonal anti-PTB serum abolished translation initiation (Fig. 6A), while normal serum or nonspecific antibodies had no such effect. This observation lends support to the notion that PTB plays a key role in cap-independent translation. Immunodepletion of PTB from cell lysates did not restore translational efficiency after reconstitution with recombinant PTB, suggesting the removal of PTB and PTB-associated factors, which may constitute important protein complexes that are essential components of internal initiation of translation. This observation is consistent with previous results with picornavirus 5′NCRs (19, 36). Furthermore, the observation that the splicing activities of poly(U)-depleted nuclear

extracts were restored only by supplementing PTB with a 100-kDa protein factor supports the results presented here (33).

The mechanism by which the HCV IRES element or those of picornaviruses recruits the 40S ribosomal subunit to form an initiation complex remains elusive. On the basis of previous studies of picornavirus IRES elements, the following have been predicted. (i) Ribosomes directly land at the IRES element by interaction of ribosomal proteins with 5′NCRs. (ii) Ribosomal subunits are recruited by *trans*-acting cellular factors that interact with 5′NCR. (iii) A characteristic, Yn-Xm-AUG motif may provide a Shine-Dalgarno sequence-like motif for the interaction of IRES with complementary sequence of 18S rRNA. A considerable level of sequence complementarity has been noted between the 3′ border of the picornavirus IRES elements and the 18S rRNA (35). A potential 18S rRNA binding site has also been localized between nt 192 and 203 of HCV 5′NCR. These sequences are complementary to bases 461 to 471 of human 18S RNA (6). Mutations introduced in these sequences of HCV exhibit no inhibitory effect on HCV IRES activity (47). While molecular mechanisms underlying PTB interaction are not clearly understood, PTB's absolute requirement in translation initiation for picornaviruses and HCV invokes an essential functional role. Possible roles of PTB could include serving as a nucleation site for general initiation factors, mediating ribosome binding, and facilitating direct binding of ribosomes and other factors by modulating the structure of the IRES (19, 22, 36). These appear to be the essential molecular interactions for the assembly of the translation initiation complex.

In summary, the present analysis unambiguously demonstrates a functional role of PTB and PTB-associated factors via physical interactions at multiple sites within the 5′NCR in the internal initiation of translation of the HCV RNA genome.

ACKNOWLEDGMENTS

We thank M. A. Garcia-Blanco for GST-2TK/PTB plasmid and polyclonal anti-PTB serum and G. Dreyfuss for monoclonal anti-PTB antibody (7G12). We also thank Peter Sarnow for constant help throughout the course of this study.

A.S. received a grant from the Lucille P. Markey Charitable Trust. N.A. received support from the Colorado Advanced Technology Institute.

REFERENCES

1. **Agol, V. I.** 1991. The 5′-untranslated region of picornaviral genomes. Adv. Virus Res. **40:**103–180.
2. **Ali, N., C. Wang, and A. Siddiqui.** Translation of HCV RNA genome. *In* Proceedings of the 25th Tokyo Princess Takamatsu Symposium on HCV and Hepatocellular Carcinoma, in press.
3. **Borman, A., M. T. Howell, J. G. Patton, and R. J. Jackson.** 1993. The involvement of a spliceosome component in internal initiation of human rhinovirus RNA translation. J. Gen. Virol. **74:**1775–1788.
4. **Borovjagin, A. V., M. V. Ezrokhi, V. M. Rostapshov, T. Y. Ugarova, T. F. Bystrova, and I. N. Shatsky.** 1991. RNA-protein interactions within the internal translation initiation region of encephalomyocarditis virus RNA. Nucleic Acids Res. **19:**4999–5005.
5. **Bothwell, A. M., D. W. Ballard, W. M. Philbrick, G. Lindwall, S. E. Maher, M. M. Bridgett, S. F. Jamison, and M. A. Garcia-Blanco.** 1991. Murine polypyrimidine tract binding protein: purification, cloning, and mapping of the RNA binding domain. J. Biol. Chem. **266:**24657–24663.
6. **Brown, E. A., H. Zhang, L.-H. Ping, and S. M. Lemon.** 1992. Secondary structure of the 5′nontranslated regions of hepatitis C virus and pestivirus genomic RNAs. Nucleic Acids Res. **20:**5041–5045.
7. **Bukh, J., R. H. Purcell, and R. H. Miller.** 1992. Sequence analysis of the 5′ noncoding region of hepatitis C virus. Proc. Natl. Acad. Sci. USA **89:**4942–4946.
8. **Chang, K. H., E. A. Brown, and S. M. Lemon.** 1993. Cell type-specific proteins which interact with the 5′ nontranslated region of hepatitis A virus RNA. J. Virol. **67:**6716–6725.
9. **Choo, Q.-L., L. K. Richman, J. H. Han, K. Berger, C. Lee, C. Dong, C. Gallegos, D. Coit, A. Medina-Selby, P. J. Barr, A. J. Weiner, D. W. Bradly, G. Kuo, and M. Houghton.** 1991. Genetic organization and diversity of the hepatitis C virus. Proc. Natl. Acad. Sci. USA **88:**2451–2455.
10. **de Wet, J. R., K. V. Wood, M. DeLuca, D. R. Helinski, and S. Subramani.** 1987. Firefly luciferase gene: structure and expression in mammalian cells. Mol. Cell. Biol. **7:**725–737.
11. **Dignam, J. D.** 1990. Preparation of extracts from higher eukaryotes, p. 194–203. *In* M. P. Deutscher (ed.), Guide to protein purification. Academic Press, Inc., New York.
12. **Ehrenfeld, E., and J. G. Gebhard.** 1994. Interaction of cellular proteins with the poliovirus 5′ noncoding region. Arch. Virol. Suppl. **9:**269–277.
13. **Garcia-Blanco, M. A., S. F. Jamison, and P. A. Sharp.** 1989. Identification and purification of a 62,000-dalton protein that binds specifically to the polypyrimidine tract of introns. Genes Dev. **3:**1874–1886.
14. **Ghetti, A., S. Pinol-Roma, W. M. Michael, C. Morandi, and G. Dreyfuss.** 1992. hnRNP I, the polypyrimidine tract-binding protein: distinct nuclear localization and association with hnRNAs. Nucleic Acids Res. **20:**3671–3678.
15. **Gil, A., P. A. Sharp, S. F. Jamison, and M. A. Garcia-Blanco.** 1991. Characterization of cDNAs encoding the polypyrimidine tract-binding protein. Genes Dev. **5:**1224–1236.
16. **Hambidge, S. J., and P. Sarnow.** 1992. Translational enhancement of the poliovirus 5′ noncoding region mediated by virus-encoded polypeptide 2A. Proc. Natl. Acad. Sci. USA **89:**10272–10276.
17. **Han, J. H., V. Shyamala, K. H. Richman, M. J. Brauer, B. Irvine, M. S. Urdea, P. Tekamp-Olson, G. Kuo, Q.-L. Choo, and M. Houghton.** 1991. Characterization of the terminal regions of hepatitis C viral RNA: identification of conserved sequences in the 5′ untranslated region and poly(A) tails at the 3′ end. Proc. Natl. Acad. Sci. USA **88:**1711–1715.
18. **Hellen, C. U. T., T. V. Pestova, M. Litterst, and E. Wimmer.** 1994. The cellular polypeptide p57 (pyrimidine tract-binding protein) binds to multiple sites in the poliovirus 5′ nontranslated region. J. Virol. **68:**941–950.
19. **Hellen, C. U. T., G. W. Witherell, M. Schmid, S. H. Shin, T. V. Pestova, A. Gil, and E. Wimmer.** 1993. A cytoplasmic 57-kDa protein that is required for translation of picornavirus RNA by internal ribosomal entry is identical to the nuclear pyrimidine tract-binding protein. Proc. Natl. Acad. Sci. USA **90:**7642–7646.
20. **Houghton, M., A. Weiner, J. Han, G. Kuo, and Q.-L. Choo.** 1991. Molecular biology of the hepatitis C viruses: implication for diagnosis, development and control of viral disease. Hepatology **14:**381–388.
21. **Jackson, R. J., M. T. Howell, and A. Kaminiski.** 1990. The novel mechanism of initiation of picornavirus RNA translation. Trends Biochem. Sci. **15:**477–483.
22. **Jang, S. K., and E. Wimmer.** 1990. Cap-independent translation of encephalomyocarditis virus RNA: structural elements of the internal ribosomal entry site and involvement of a cellular 57-kDa RNA-binding protein. Genes Dev. **4:**1560–1572.
23. **Kato, N., M. Hijikata, Y. Ootsuyama, M. Nakagawa, S. Ohkoshi, T. Sugimura, and K. Shimotohno.** 1990. Molecular cloning of the human hepatitis C virus genome from Japanese patients with non-A non-B hepatitis. Proc. Natl. Acad. Sci. USA **87:**9524–9528.
24. **Kettinen, H., K. Grace, S. Grunert, B. Klarke, D. Rowlands, and R. Jackson.** 1994. Mapping of the internal ribosome entry site at the 5′ end of the hepatitis C virus genome, p. 125–131. *In* K. Nishioka, H. Suziki, S. Mishiro, and T. Oda. (ed.), Proceedings of the International Symposium on Viral Hepatitis and Liver Disease, Tokyo.
25. **Kozak, M.** 1989. The scanning model for translation: an update. J. Cell Biol. **108:**229–241.
26. **Luz, N., and E. Beck.** 1991. Interaction of a cellular 57-kilodalton protein with the internal translation initiation site of foot-and-mouth disease virus. J. Virol. **65:**6486–6494.
27. **Macejak, D. G., and P. Sarnow.** 1991. Internal initiation of translation mediated by 5′ leader of a cellular mRNA. Nature (London) **353:**90–94.
28. **Meerovitch, K., Y. V. Svitkin, H. S. Lee, F. Lejbkowicz, D. J. Kenan, E. K. L. Chan, V. I. Agol, J. D. Keene, and N. Sonenberg.** 1993. La autoantigen enhances and corrects aberrant translation of poliovirus RNA in reticulocyte lysate. J. Virol. **67:**3798–3807.
29. **Miller, R. H., and R. H. Purcell.** 1990. Hepatitis C virus shares amino acid sequence similarity with pestiviruses and flaviviruses as well as members of two plant virus supergroups. Proc. Natl. Acad. Sci. USA **87:**2057–2061.
30. **Mulligan, G. J., W. Guo, S. Wormsley, and D. M. Helfman.** 1992. Polypyrimidine tract binding protein interacts with sequences involved in alternative splicing of β-tropomyosine pre-mRNA. J. Biol. Chem. **267:**25480–25487.
31. **Oh, S.-K., M. P. Scott, and P. Sarnow.** 1993. Homeotic gene antinnapedia mRNA contains 5′-noncoding sequences that confer translational initiation by internal ribosome binding. Genes Dev. **6:**1643–1653.
32. **Okamoto, H., S. Okada, Y. Sugiyama, K. Kurai, H. Iizuka, A. Machida, Y. Miyakawa, and M. Mayumi.** 1991. Nucleotide sequence of the genomic RNA of hepatitis C virus isolated from a human carrier: comparison with reported isolates for conserved and divergent regions. J. Gen. Virol. **72:**2697–2704.
33. **Patton, J. G., S. A. Mayer, P. Tempst, and B. Nadal-Ginard.** 1991. Characterization and molecular cloning of polypyrimidine tract-binding protein: a component of a complex necessary for pre-mRNA splicing. Genes Dev. **5:**1237–1251.

34. **Pestova, T. V., C. U. T. Hellen, and E. Wimmer.** 1991. Translation of poliovirus RNA: role of an essential *cis*-acting oligopyrimidine element within the 5′ nontranslated region and involvement of a cellular 57-kilodalton protein. J. Virol. **65:**6194–6204.
35. **Pilipenko, E. V., A. P. Gmyl, S. V. Maslova, Y. V. Svitkin, A. N. Sinyakov, and V. I. Agol.** 1992. Prokaryotic-like cis elements in the cap-independent internal initiation of translation on picornavirus RNA. Cell **68:**119–131.
36. **Schmid, M., and E. Wimmer.** 1994. IRES-controlled protein synthesis and genome replication of poliovirus. Arch. Virol. Suppl. **9:**279–289.
37. **Sherlock, D. S.** 1993. Viral hepatitis C. Curr. Opin. Gasteroenterol. **9:**341–348.
38. **Sonenberg, N.** 1990. Poliovirus translation. Curr. Top. Microbiol. Immunol. **161:**23–47.
39. **Stade, K., J. Rinke-Appel, and R. Brimacombe.** 1989. Site-directed cross-linking of mRNA analogues to the *Escherichia coli* ribosome; identification of 30S ribosomal components that can be cross-linked to the mRNA at various points 5′ with respect to the decoding site. Nucleic Acids Res. **17:**9889–9908.
40. **Svitkin, Y. V., K. Meerovitch, H. S. Lee, J. N. Dholakia, D. J. Kenan, V. I. Agol, and N. Sonenberg.** 1994. Internal translation initiation on poliovirus RNA: further characterization of La function in poliovirus translation in vitro. J. Virol. **68:**1544–1550.
41. **Takamizawa, A., C. Mori, I. Fuke, S. Manabe, S. Murakami, J. Fujita, E. Onishi, T. Andoh, I. Yoshida, and H. Okayama.** 1991. Structure and organization of the hepatitis C virus genome isolated from human carriers. J. Virol. **65:**1105–1113.
42. **Tsukiyama-Kohara, K., N. Iizuka, M. Kohara, and A. Nomoto.** 1992. Internal ribosome entry site within hepatitis C virus RNA. J. Virol. **66:**1476–1483.
43. **Tsukuma, H., T. Hiyama, S. Tanaka, M. Nakao, T. Yabuuchi, T. Kitamura, K. Nakanishi, I. Fujimoto, A. Inoue, H. Yamazaki, and T. Kawashima.** 1993. Risk factors for hepatocellular carcinoma among patients with chronic liver disease. N. Engl. J. Med. **328:**1797–1801.
44. **Wakita, T., and J. R. Wands.** 1994. Specific inhibition of hepatitis C virus expression by antisense oligodeoxynucleotides: *in vitro* model for selection of target sequence. J. Biol. Chem. **269:**14205–14210.
45. **Wang, C., S.-Y. Le, N. Ali, and A. Siddiqui.** 1995. An RNA pseudoknot is essential for internal initiation of translation of the hepatitis C virus RNA genome. RNA **1:**526–537.
46. **Wang, C., P. Sarnow, and A. Siddiqui.** 1993. Translation of human hepatitis C virus RNA in cultured cells is mediated by an internal ribosome-binding mechanism. J. Virol. **67:**3338–3344.
47. **Wang, C., P. Sarnow, and A. Siddiqui.** 1994. A conserved helical element is essential for internal initiation of translation of hepatitis C virus RNA. J. Virol. **68:**7301–7307.
48. **Wang, C., and A. Siddiqui.** 1995. Structure and function of the hepatitis C virus internal ribosome entry site. Curr. Top. Microbiol. **203:**99–115.
49. **Witherell, G. W., A. Gill, and E. Wimmer.** 1993. Interaction of polypyrimidine tract binding protein with the encephalomyocarditis virus mRNA internal ribosome entry site. Biochemistry **32:**8268–8275.
50. **Witherell, G. W., and E. Wimmer.** 1994. Encephalomyocarditis virus internal ribosomal entry site RNA-protein interactions. J. Virol. **68:**3183–3193.